Materials Letters 105 (2013) 36–39

Contents lists available at SciVerse ScienceDirect

Materials Letters

journal homepage: www.elsevier.com/locate/matlet

Fe_3O_4@Pt nanoparticles with enhanced peroxidase-like catalytic activity

Ming Ma [a], Jun Xie [a], Yu Zhang [a], Zhongping Chen [b], Ning Gu [a,*]

[a] State Key Laboratory of Bioelectronics, Jiangsu Key Laboratory of Biomaterials and Devices, Southeast University, Nanjing 210009, People's Republic of China
[b] Institute of Nautical Medicine, Nantong University, Nantong 226001, People's Republic of China

ARTICLE INFO

Article history:
Received 13 November 2012
Accepted 6 April 2013
Available online 12 April 2013

Keywords:
Nanocomposites
Biomaterials
Magnetite
Platinum
Peroxidase

ABSTRACT

Pt modified Fe_3O_4 magnetic nanoparticles (Fe_3O_4@Pt NPs) were synthesized by a simple method. The morphology and crystal structure of the as-prepared nanocomposite were characterized by TEM, XRD and EDS. The peroxidase-like catalytic activity of the synthesized nanoparticles was also investigated. Catalysis was found to follow Michaelis–Menten kinetics. The calculated kinetic parameters of the Fe_3O_4@Pt NPs show that they exhibited strong affinity with substrates and enhanced catalytic activity than that of Fe_3O_4 nanoparticles, suggesting a higher peroxidase-like activity.

1. Introduction

Nanostructured magnetic materials have aroused extensive attention mainly in biomedical applications, including protein immobilization and separation, targeted drug delivery, cancer hyperthermia treatments, contrast enhancement agents for magnetic resonance imaging (MRI), and so on [1]. Recently, it was also reported that Fe_3O_4 nanoparticles (NPs) could possess intrinsic peroxidase-like activity [2,3]. This surprising finding makes magnetic Fe_3O_4 NPs have a wide range of potential application in chemical catalysis and biomedical detection. When replacing horseradish peroxidase (HRP), the Fe_3O_4 NPs exhibit superior performances in traditional enzyme linked immunosorbent assay (ELISA) and other bio-detections with advantages of controlled synthesis at low cost, tunability in catalytic activities, and high stability against stringent conditions [2].

Recently, several authors have reported on the magnetic iron or iron oxide NPs coated with a metallic shell [4,5]. The core–shell types of iron oxide NPs, owing to inner iron oxide core with an outer metallic shell of inorganic materials, not only provided stability of the nanoparticles in solution but also helped in various biomedical applications. Numerous materials have been used to modify the surface of Fe_3O_4 nanoparticles, especially Au and Ag. As a super-catalyst, Pt NPs have been extensively explored for applications in fuel cells, hydrogenation, and air purification [6,7]. Sun's [8] and Schaak's [9] groups synthesized colloidal Pt–Fe_3O_4 heterodimers (dumbbell-like) by epitaxial growth of Fe onto Pt seed particles followed by Fe oxidation. The Pt–Fe_3O_4 NPs exhibited a 20-fold increase in mass catalytic activity toward oxygen reduction reaction compared with the single component Pt NPs [8]. Xu's group prepared a kind of Fe_3O_4/SiO_2 magnetic hybrids, and then loaded Pt, Au, and Pd nanocatalysts on the surface [10]. The magnetic hybrid-supported noble metal nanocatalysts were found to have high catalytic activity in reduction of 4-nitrophenol, alcohol oxidation, and the Heck reaction, and could be readily recycled by an external magnet because of their magnetic support. Recently, small Pt NPs have been suggested to act as a potent peroxidase mimic [11,12]. We envisaged that when modified with Pt, based on the excellent catalytic property of Pt, as well as on the superparamagnetism and peroxidase-like property of Fe_3O_4, the resultant nanocomposites might show both superparamagnetism and enhanced peroxidase-like activity. Thus, we presented a simple approach to synthesize nanocomposite Pt modified Fe_3O_4 NPs (simplified as Fe_3O_4@Pt NPs). Furthermore, we investigated the peroxidase-like activities of the Fe_3O_4@Pt NPs. The activity of Fe_3O_4@Pt NPs as peroxidase mimic was evaluated using the typical HRP substrates (TMB, 3, 3′, 5, 5′-tetramethylbenzidine) in the presence of H_2O_2.

2. Experimental

Monodisperse hydrophobic Fe_3O_4 NPs were synthesized by the known method [13]. Hydrophilic Fe_3O_4 NPs modified by DMSA (meso-2,3-dimercaptosuccinic acid) were then prepared via surface double-exchange according to our previous work [14]. The obtained DMSA modified Fe_3O_4 NPs were used in followed procedure of Pt deposition.

Deposition of Pt on Fe_3O_4 NPs was achieved by reducing the Pt salt precursor, K_2PtCl_4, in aqueous solution. In a typical experiment,

* Corresponding author. Tel.: +86 258327 2460.
E-mail address: guning@seu.edu.cn (N. Gu).

0167-577X/$ - see front matter © 2013 Elsevier B.V. All rights reserved.
http://dx.doi.org/10.1016/j.matlet.2013.04.020

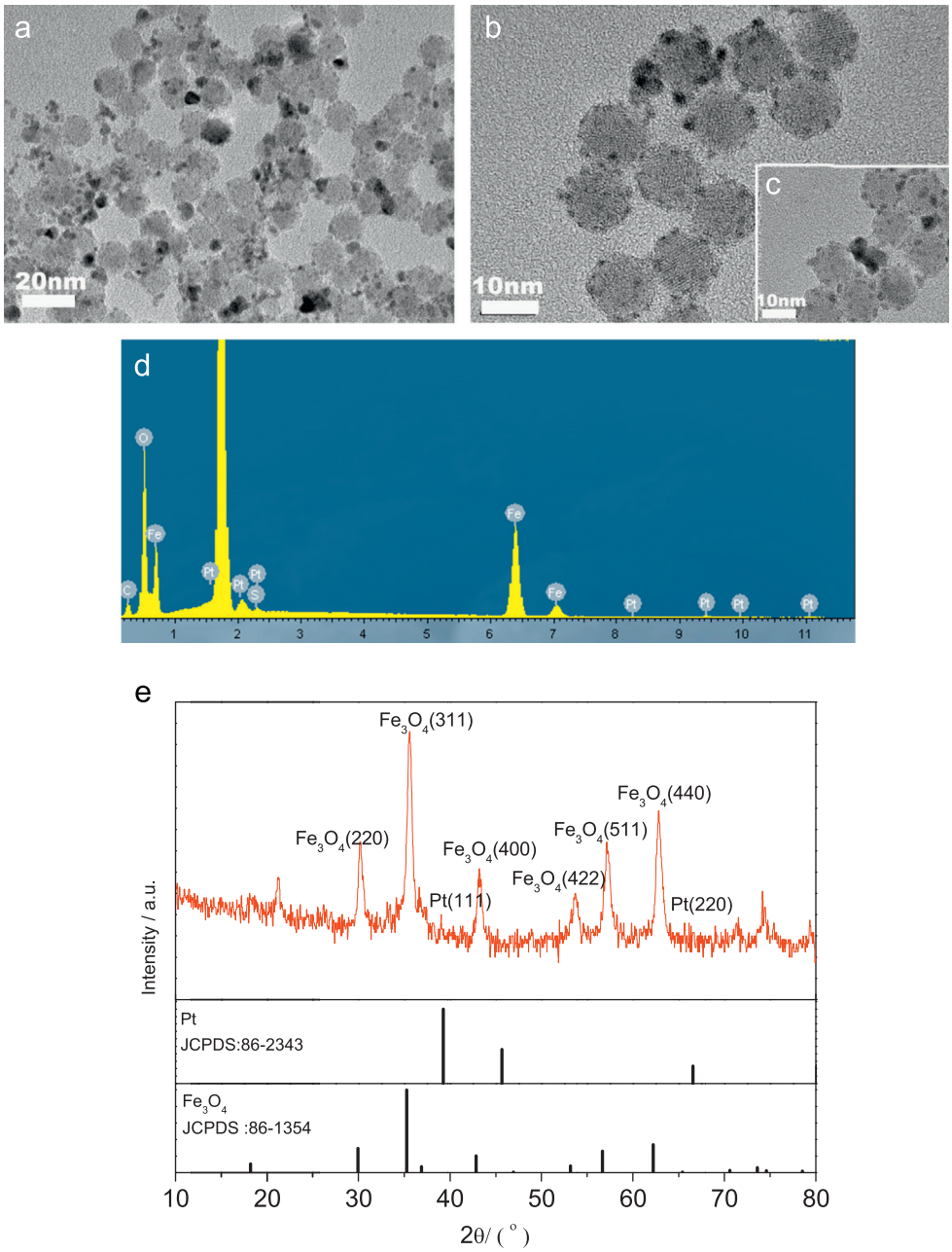

Fig. 1. (a) Low- and (b) high-magnification TEM photograph of Fe_3O_4@Pt NPs. (c) TEM photograph of Fe_3O_4@Pt NPs collected after catalysis reaction. (d) EDS analysis spectrum of Fe_3O_4@Pt NPs. (e) XRD pattern of Fe_3O_4@Pt NPs.

8 mL DMSA-Fe_3O_4 NPs aqueous solution (11 mM Fe) was taken in a 20 mL flask. The flask was then placed in an ultrasonic bath; the bath temperature was raised to 70 °C and remained the same throughout the experiment. 2 mL 0.5 mM metal precursor was added to the flask using a pipette. 0.4 mL 0.1 mol/L fresh-prepared $NaBH_4$ solution was added as a reducer after 30 min. The reduction reactions lasted for 2 h. The obtained Fe_3O_4@Pt NPs were separated by centrifugation and then washed 4 times with deionized water.

The particle morphology of the NPs obtained above was characterized by transmission electronic microscopy (TEM, JEOL JEM-2100). The structure was detected by an X'TRA X-ray diffractometer (XRD). An energy dispersive spectrometer (EDS) was used to determine the element ratio of iron and platinum.

The reaction kinetics for the catalytic oxidation of TMB was studied by recording the absorption spectra with a 30 s interval in scanning kinetics mode using multimode and absorbance microplate readers (TECAN, Infinite 200). Unless other wise stated, the reaction was carried out at room temperature with 3 μg Fe/mL Fe_3O_4 NPs or Fe_3O_4@Pt NPs in 1 mL reaction buffer (sodium citrate buffer, 0.1 M, pH 4.4) in the presence of different concentrations of TMB or H_2O_2. Catalytic parameters were determined by fitting the absorbance data to the Michaelis–Menten equation

$$v = v_{max}[S]/(K_m + [S]) \quad (1)$$

The Michaelis–Menten equation describes the relationship between the rates of substrate conversion by an enzyme and the concentration of the substrate. In this equation, v is the initial velocity, v_{max} is the maximal reaction velocity, [S] is the substrate concentration, and K_m is the Michaelis constant.

3. Results and discussion

Fig. 1a and b shows a typical morphology image of Fe_3O_4@Pt NPs. Fig. 1a is a typical large-area TEM image of the Fe_3O_4@Pt NPs, where the core and shell components can be easily differentiated by brightness differences. Additional structural details are revealed by a higher resolution TEM image in Fig. 1b. The TEM image shows that the particles are well-distributed Pt nanodots (diameter ca. 2 nm) with rather uniform size on the Fe_3O_4 core. Fig. 1c is a TEM image of the Fe_3O_4@Pt NPs collected after catalysis reaction. Compared with Fig. 1b, the morphology of the Fe_3O_4@Pt NPs had not changed obviously after the catalysis reaction with TMB and H_2O_2. The chemical composition of Fe_3O_4@Pt NPs (randomly chosen) was analyzed by EDS. As shown in Fig. 1d, the atom proportion of Fe:Pt is 19.4:1 with a bit lower than inputs.

Powder XRD patterns of Fe_3O_4@Pt NPs are shown in Fig. 1e. The positions and relative intensities of peaks observed at 2θ of 30.17°, 35.54°, 43.27°, 53.62°, 57.11° and 62.85° match perfectly to Fe_3O_4 with the cubic inverse spinel structure according to JCPDS 86-1354 card. Diffraction peaks at 2θ of 39.06°, 49.23°, and 65.91° correspond well to Pt (JCPDS 86-2343).

The peroxidase-like behavior of the synthesized NPs was examined using TMB as a chromogenic substrate. TMB has been proved to be a noncarcinogenic derivative and can be oxidized to a blue reaction product with maximum absorbance at 370 and 650 nm in the presence of H_2O_2. Fig. 2 shows the UV–vis absorption spectra of the catalytic reaction systems upon reaction for 15 min after adding Fe_3O_4 or Fe_3O_4@Pt NPs solution to the working solution. As shown in Fig. 2, two peaks are observed at 369 and 652 nm, indicating that TMB was oxidized. We can see that Fe_3O_4@Pt NPs as peroxidase mimic exhibit a stronger absorbance than that of Fe_3O_4 NPs.

A kinetic investigation of oxidation of TMB was performed by measuring the absorbance at 652 nm as a function of time after adding Fe_3O_4 or Fe_3O_4@Pt NPs solution to the working solution. Fig. 3a presents the time course curves of the reaction systems catalyzed by Fe_3O_4 and Fe_3O_4@Pt NPs within 15 min. Absorbance data were back-calculated to concentration by the Beer–Lambert Law using a molar absorption coefficient of 39000 M^{-1} cm^{-1} for TMB-derived oxidation products [3]. Apparent steady state reaction rates at different concentrations of substrate were obtained by calculating the slopes of initial absorbance changes with time. Data shown in Fig. 3b and c were fit to the Michaelis–Menten

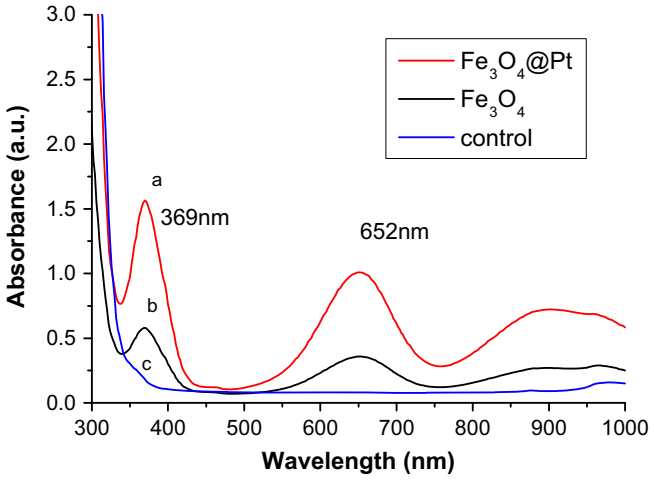

Fig. 2. UV–vis absorption spectra of the sodium citrate buffer (pH=4.4) containing 0.5 M H_2O_2 and 0.5 mM TMB in the presence of (a) Fe_3O_4@Pt NPs and (b) Fe_3O_4 NPs with equal concentration of Fe (3 μg/mL). The same reaction system without NPs as catalyst was also used as a control (c).

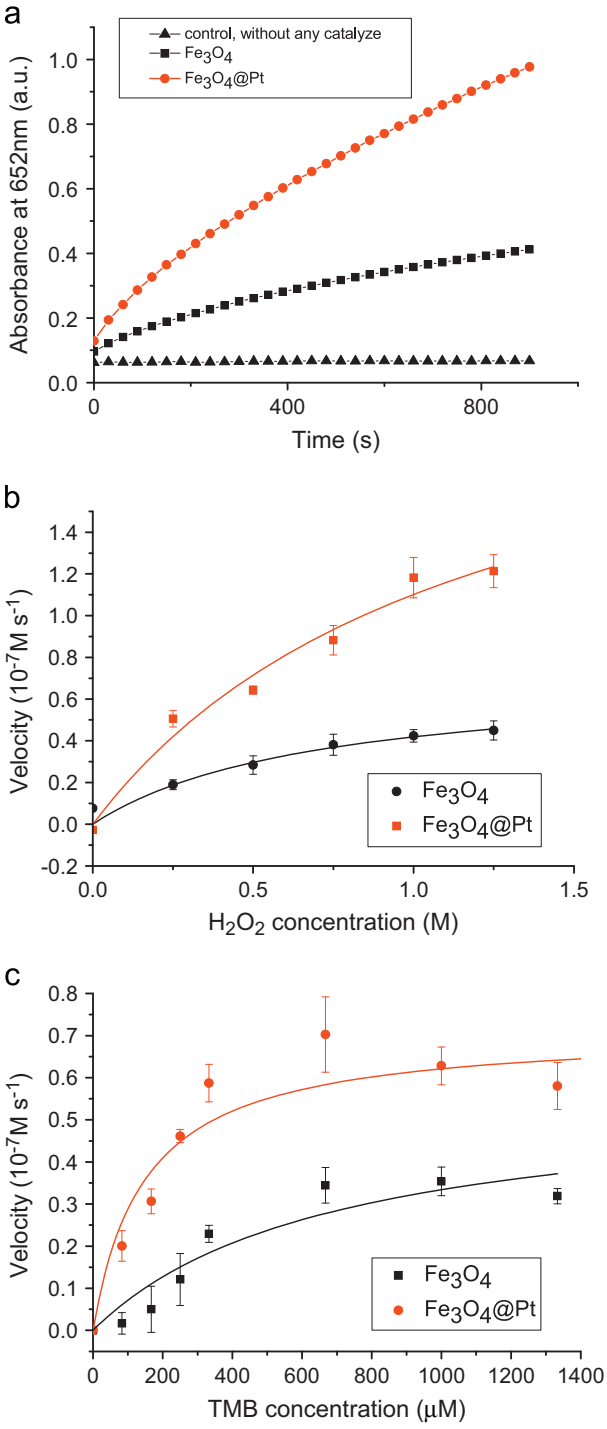

Fig. 3. (a) UV–vis absorbance–time course curves of TMB–H_2O_2 reaction system (1 mL 0.1 M sodium citrate buffer in the presence of 1 M H_2O_2 and 0.5 mM TMB). (b) The reaction rate of different NPs in TMB–H_2O_2 reaction system with different concentrations of H_2O_2 and (c) TMB.

equation and model parameters (v_{max} and K_m) extracted. The catalytic constant (k_{cat}: v_{max} normalized for enzyme content) was also calculated [3]:

$$k_{cat} = v_{max}/[E] \quad (2)$$

where [E] was taken as the nanoparticle or enzyme concentration. Catalytic parameters are summarized in Table 1. Michaelis constant (K_m) measures the concentration of substrate at which the reaction reaches ½v_{max}. This is an important parameter to measure binding affinity of the enzyme to the substrate, and can be applied

Table 1
Apparent kinetic parameters of Fe_3O_4 and Fe_3O_4@Pt NPs as both peroxidase mimetics. K_m is the Michaelis constant, v_{max} is the maximal reaction velocity and k_{cat} is the catalytic constant, where $k_{cat} = v_{max}/[E]$. $[E]$ is nanoparticle concentration. Here, $[E] = 8.453 \times 10^{-10}$ M. The k_{cat} value shows the catalytic efficiency per nanoparticle.

	Substrate	K_m (mM)	v_{max} M s^{-1}	k_{cat} s^{-1}	k_{cat}/K_m (M^{-1} s^{-1})
Fe_3O_4	TMB	0.485	0.563×10^{-7}	66.604	1.373×10^5
	H_2O_2	1175.3	2.396×10^{-7}	28.345	2.412×10^2
Fe_3O_4@Pt	TMB	0.147	0.711×10^{-7}	84.112	5.722×10^5
	H_2O_2	702.6	7.136×10^{-7}	84.420	1.202×10^3

similarly here to study NP–TMB interaction. We can see that K_m from the Fe_3O_4@Pt NPs is only half the value of that from the Fe_3O_4 NPs, indicating that the Fe_3O_4@Pt NPs have a much higher affinity to TMB. This is likely attributed to the enhanced binding between Pt particles and TMB by Pt–NH_2 interaction. As a result, Fe_3O_4@Pt NPs exhibit a larger k_{cat} value than that of Fe_3O_4 NPs, suggesting a higher peroxidase-like activity.

4. Conclusion

Platinum modified Fe_3O_4 nanoparticles were prepared by a simple method and characterized by TEM, XRD and EDS. The surface Pt nanoparticle coating increases affinity for substrate of TMB and thus the resultant composite nanoparticles show a synergistic effect for enhanced catalytic oxidation of TMB by H_2O_2 and can serve as a high-efficiency peroxidase mimic.

Acknowledgment

This research was supported by the National Important Science Research Program of China (No. 2011CB933503), the National Natural Science Foundation of China (Nos. 30970787 and 31170959), Research Fund for the Doctoral Program of Higher Education of China (20110092110029).

References

[1] Ruiz-Hernández E, Baeza A, Vallet-Regí M. ACS Nano 2011;5(2):1259–66.
[2] Gao L, Zhuang J, Nie L, Zhang J, Zhang Y, Gu N, et al. Nat Nanotechnol 2007;2:577–83.
[3] Zhang XQ, Gong SW, Zhang Y, Yang T, Wang CY, Gu N. J Mater Chem 2010;20:5110–6.
[4] Xie HY, Zhen R, Wang B, Feng YJ, Chen P, Hao J. J Phys Chem C 2010;114 (11):4825–30.
[5] Du J, Jing C. J Phys Chem C 2011;115(36):17829–35.
[6] Wu B, Huang H, Yang J, Zheng N, Fu G. Angew Chem 2012;124(14):3496–9.
[7] Kibsgaard J, Gorlin Y, Chen Z, Jaramillo TF. J Am Chem Soc 2012;134 (18):7758–65.
[8] Wang C, Daimon H, Sun S. Nano Lett 2009;9(4):1493–6.
[9] Buck MR, Bondi JF, Schaak RE. Nat Chem 2012;4:37–44.
[10] Zhou L, Gao C, Xu W. Langmuir 2010;26(13):11217–25.
[11] He W, Liu Y, Yuan J, Yin JJ, Wu X, Hu X, et al. Biomaterials 2011;32:1139–47.
[12] Ma M, Zhang Y, Gu N. Colloids Surf A 2011;373(1–3):6–10.
[13] Park J, An K, Hwang Y, Park JG, Noh HJ, Kim JY, et al. Nat Mater 2004;3:891–5.
[14] Chen ZP, Zhang Y, Xu K, Xu RZ, Liu JW, Gu N. J Nanosci Nanotechnol 2008;8:6260–5.